JOURNAL OF THE ROYAL SOCIETY Interface

rsif.royalsocietypublishing.org

Research

Cite this article: Wang L, Brodbeck L, Iida F. 2014 Mechanics and energetics in tool manufacture and use: a synthetic approach. *J. R. Soc. Interface* **11**: 20140827.
http://dx.doi.org/10.1098/rsif.2014.0827

Received: 25 July 2014
Accepted: 20 August 2014

Subject Areas:
biomimetics, computational biology, bioenergetics

Keywords:
tool manufacture and use, phenotypic plasticity, biomechanics, energy, robot

Author for correspondence:
Liyu Wang
e-mail: liyu.wang@mavt.ethz.ch

Electronic supplementary material is available at http://dx.doi.org/10.1098/rsif.2014.0827 or via http://rsif.royalsocietypublishing.org.

Royal Society Publishing

Mechanics and energetics in tool manufacture and use: a synthetic approach

Liyu Wang, Luzius Brodbeck and Fumiya Iida

Bio-Inspired Robotics Lab, Institute of Robotics and Intelligent Systems, ETH Zurich, Leonhardstrasse 27, Zurich 8092, Switzerland

Tool manufacture and use are observed not only in humans but also in other animals such as mammals, birds and insects. Manufactured tools are used for biomechanical functions such as effective control of fluids and small solid objects and extension of reaching. These tools are passive and used with gravity and the animal users' own energy. From the perspective of evolutionary biology, manufactured tools are extended phenotypes of the genes of the animal and exhibit phenotypic plasticity. This incurs energetic cost of manufacture as compared to the case with a fixed tool. This paper studies mechanics and energetics aspects of tool manufacture and use in non-human beings. Firstly, it investigates possible mechanical mechanisms of the use of passive manufactured tools. Secondly, it formulates the energetic cost of manufacture and analyses when phenotypic plasticity benefits an animal tool maker and user. We take a synthetic approach and use a controlled physical model, i.e. a robot arm. The robot is capable of additively manufacturing scoop and gripper structures from thermoplastic adhesives to pick and place fluid and solid objects, mimicking primates and birds manufacturing tools for a similar function. We evaluate the effectiveness of tool use in pick-and-place and explain the mechanism for gripper tools picking up solid objects with a solid-mechanics model. We propose a way to formulate the energetic cost of tool manufacture that includes modes of addition and reshaping, and use it to analyse the case of scoop tools. Experiment results show that with a single motor trajectory, the robot was able to effectively pick and place water, rice grains, a pebble and a plastic box with a scoop tool or gripper tools that were manufactured by itself. They also show that by changing the dimension of scoop tools, the energetic cost of tool manufacture and use could be reduced. The work should also be interesting for engineers to design adaptive machines.

1. Introduction

Tool use by non-human animals has been defined in a variety of ways [1,2], and the number of species that can be said to be exhibiting tool use varies depending on the exact definition used [3]. According to Bentley-Condit & Smith [1], tool use is widespread across three phyla and seven classes of the animal kingdom. Compared to mere tool use, tool manufacture and use is rarer (ch. 4 in [4]) and was once thought to be a unique behaviour and capability of humans. According to a definition by Shumaker *et al*. (ch. 1, p. 11 in [2]), tool manufacture is any structural modification of an object or an existing tool so that the object serves, or serves more effectively, as a tool. Manufactured tools are a type of animal-built structures, alongside homes, foraging structures and communication structures (ch. 1 in [4]). Animal-built structures such as nests, burrows, traps and webs are not manufactured tools because once completed they are not held or directly manipulated in their entirety (ch. 7, p. 204 in [2]).

It is now clear that several classes of non-human animals manufacture and use tools. Tool manufacture behaviour is present in primates and other mammals, birds, insects and Malacostraca [1,2]. As exemplified in figure 1, rooks

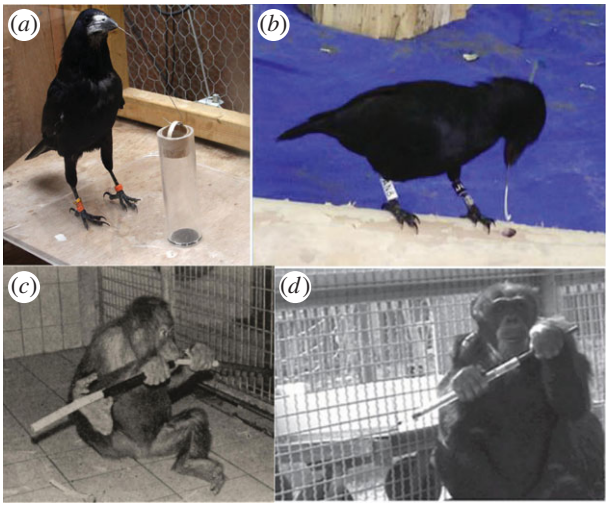

Figure 1. Examples of tool manufacture and use in non-human animals. (*a*) Rooks can bend a straight piece of wire into a hook to extract a bucket from a vertical tube; (*b*) New Caledonian crows can collect tree leaves and twigs to make hooks for extraction of food from cracks and holes; (*c*) orangutans and (*d*) chimpanzees are capable of collecting materials and combining them into simple tools to extend reaching. (*a*) Adapted from [5]. Copyright © The National Academy of Sciences of the United States of America. (*b*,*d*) Adapted from [6,7]. Copyright © The Royal Society. (*c*) Adapted from [8] Copyright © E. Schweizerbart'sche Verlagsbuchhandlung. (Online version in colour.)

can bend a straight piece of wire into a hook to extract a bucket from a vertical tube; New Caledonian crows can collect tree leaves and twigs to make hooks for extraction of food from cracks and holes; orangutans and chimpanzees are capable of collecting materials and combining them into simple tools.

Tool manufacture takes four modes: detach, subtract, add/combine and reshape (ch. 1, p. 16 in [2]). All the four modes have one single function which is to make an object serve more effectively as a tool (ch. 1, p. 17 in [2]). Then the manufactured tool serves several functions for the animal user. Shumaker *et al*. categorized seven such functions according to motorical descriptions, including to create or augment signal value of social display, to amplify mechanical force, to extend user's reach, to hide or camouflage the user, to provide or enhance bodily comfort for the user, to effectively control fluids and small solid objects and to abstract or represent reality (ch. 1, pp. 17–18 in [2]).

A common feature of tool manufacture and use in animals is that they power their tools only with gravity and their own energy (last ch. in [2]). In other words, all manufactured tools by non-human animals are passive. As tool functions include categories related to mechanics such as force amplification, extension of reaching and control of fluids and small solid objects, the first goal of this paper is to investigate possible underlying mechanical mechanisms of the use of passive manufactured tools.

Manufactured tools are extended phenotypes [9] of the genes of an animal and they exhibit phenotypic plasticity [10]. For example, New Caledonian crows make and use two types of hook structures depending on the environment the prey is located: a hook structure made from twig is usually held angleways in a crow's bill in the base of leaves and in the broken-off ends of dead branches, and a stepped-cut tool from a flat, narrow section of pandanus leaf edge is usually held lengthways in the bill [11,12]. New Caledonian crows were also found to manufacture during use, a tool of a suitable diameter from a tree branch, according to the diameter of the hole through which the tool would have to be inserted [13]. Sumatran orangutans make and use different tools from tree branches for insect foraging and fruigivory, whereas the bark of fruit tools was always removed, this was variable among the insect foraging tools [14].

Phenotypic plasticity incurs cost [15] which was defined as a reduction in the fitness as a consequence of expressing a certain phenotype through plastic rather than fixed development [16]. According to Dewitt *et al*. [17], five kinds of costs of phenotypic plasticity may be defined, including production costs. Production costs of plasticity in manufactured tools include but are not limited to: the energetic costs of collecting additional materials and the energetic cost of manufacture of several tools; and additional expression costs, e.g. extended phenotypes may make an animal more/less conspicuous to predators/potential mates/conspecifics, etc. The second goal of this paper is to find a way to formulate the energetic cost of manufacture and analyse when phenotypic plasticity brings benefits to an individual animal that makes and uses different tools.

To investigate the above two topics related to mechanics and energetics, we take a synthetic approach and use a controlled physical model which is a stationed robot. Robots have been used to study locomotion biomechanics [18–23], neural control strategies [24–26] and animal behaviours [27,28]. The robots are often reduced-order models of the animals with similarities in certain aspects that are of the interest to investigation. Here, the robot mimics the add/combine mode and the reshape mode of tool manufacture for more effective control of fluids and solid objects. Such behaviours were found in birds including New Caledonian crows, American crows and rooks, as well as primates such as capuchin monkeys, orangutans, gorillas, bonobos and chimpanzees [2].

The robot contains synthetic material thermoplastic adhesive (TPA) onboard to represent raw material collected by animals. TPA was chosen because it offers good plastic and bonding properties which can be easily controlled through temperature [29–31] for automation purposes. It has been used in robotics and automation to handle small-sized parts at the submillimetre scale [32–35] as well as in robotic locomotion [36,37]. The type of TPA used in our study (Pattex Hot Stick Transparent, Henkel, Germany) is based on copolymer ethylene vinyl acetate. It is commercially provided in cylindrical sticks (cross-sectional diameter 11.5 mm, length 204 mm). The TPA has storage modulus and tensile strength both over 10 MPa at the room temperature, a density $\rho = 970\ \mathrm{kg\ m^{-3}}$, a softening point at 60–80°C and a melting temperature at 150–170°C.

The robot employs an additive manufacturing technique for making tools for itself. The tools can be varied by modifying preloaded program for manufacture and are intended to pick and place fluid and various solid objects. Specifically, two types of tools were manufactured and used, passive grippers and scoops. Some of the passive grippers had hooks on the tips of fingers to represent hook structures manufactured by animals, whereas scoops represent water-fetching structures manufactured by animals. We evaluate the effectiveness of tool use in pick-and-place and explain the mechanism for gripper tools picking up solid objects with a solid-mechanics model. We propose a way to formulate the energetic cost of tool manufacture and use it to analyse the case of scoop tools.

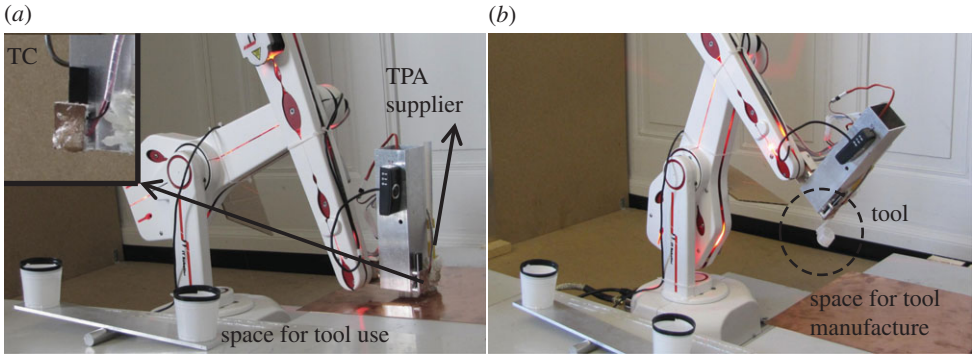

Figure 2. (*a*) A robotic arm was modified by adding a TPA Supplier and a TC and used as the controlled physical model for mechanics and energetics in the study. It is installed in front of a space for tool manufacture and a motor task space for tool use. Inset: a closer image of TC. It contains a thin copper plate, a Peltier element and a heat sink. By supplying electric current through the power cable, the Peltier element can increase temperature of the copper plate, and a change of polarity in electric current can induce a decrease in temperature. (*b*) The robot after tool manufacture (a tool shown in the dashed lined circle).

2. Material and methods

2.1. A controlled physical model

A five-axis robot arm (R12 firefly, ST Robotics, UK; apparent power 420 VA) was modified with TPA material and its handling devices onboard. As shown in figure 2, the robot arm is stationed on a flat open ground, where its reaching range covers a horizontal workspace for tool manufacture and a motor task space for tool use. The workspace is pre-coated with a thin layer of oily spray for ease of detachment of manufactured tools. At the end, effector of the robot arm, two TPA handling devices are added based on our previous development [38,39]. One of the devices is called TPA Supplier and it controlled the deposition of heated and melted TPA for building structures. The device heats the solid TPA stick and pushes it through a nozzle with a position-controlled servomotor. With a power consumption of 15 W, the device can maintain the temperature of the TPA at 150°C. The other device is called thermal connector (TC) and it has a copper surface (20 × 20 mm) that can be heated and cooled by a Peltier element (TEC1-01703, Centenary Materials, China; power 4 W). By regulating the electric current to the element, the copper surface is capable of connecting to structures made from TPA by firstly heating and softening the TPA on the surface, and subsequently cooling to form adhesive bonding. TC is capable of repeatedly and continuously increasing and decreasing the temperature between 40 and 65°C in 35 and 105 s, respectively.

The robot is controlled based on the positions of the nozzle or the centre of the TC in a global Cartesian coordinate. A Matlab script running on a desktop PC sends predefined commands to the controller box of the robot arm, and the controller computes joint angles from inverse kinematics with a time interval of 20 ms. Heating and cooling in TPA Supplier and TC are controlled through a micro-controller (Duemilanove, Arduino, Italy) through relays. More specifically, a relay is used to control the heater of TPA Supplier based on feedback from a temperature sensor (CON-TS-NTC, Hygrosens, Germany) mounted near the nozzle. Two more relays are used to control ON/OFF and direction of the electric current through the Peltier element in TC in an open-loop manner.

2.2. Fluid and solid objects

Objects to be picked and placed include fluid, solid granules and rigidly solid objects. More specifically, water was chosen as the fluid, and in terms of solids, rice grains, an irregularly shaped pebble and a plastic box were used. Seventy grams of water was poured into a rectangular-shaped container (with a top opening of approx. 45 × 60 mm and a depth of 30 mm); 140 g of rice grains with each piece weighing approximately 0.018 g with a cross-sectional diameter approximately 1 mm and a length 5 mm were contained in a rectangular tray (filled volume 80 × 90 × 20 mm). The pebble is approximately 4.0 g with a size of approximately 8 × 15 × 20 mm at the most on each dimension. The plastic box is approximately 6.6 g with a size of 30 × 30 × 85 mm. Photos of the objects can be found in figure 6.

2.3. Tool manufacture

Six passive tools were manufactured by the robot including three fingered grippers and three scoops of different sizes. The three fingered grippers will be used to verify a solid-mechanics model (further detail in §2.4) explaining the mechanics of pick-and-place, whereas the three scoops will be used to analyse the energetics of making and using tools of different sizes.

The grippers have a top bar and two fingers (two-dimensional schematics can be found later in figure 3*a*). The top bars in all grippers were narrower than 2 mm, so that they could be fully bonded with TC to assure rigidity. The grippers had different finger dimensions and initial angles between the fingers and the top bar, so that openings of finger tips can accommodate solid objects of different dimensions. The dimensions of fingers in the grippers were 3 × 15 mm, 5 × 20 mm and 5 × 60 mm, and the thickness were 1.5 mm, 5 mm and 10 mm (corresponding to grippers from the smallest opening to the largest with ID of 1–3). In the case of gripper 1, 10 fingers were used, and in the other two grippers, a rigid jaw was added to the tip of each finger.

The scoops consist of three parts, i.e. a bottom disc, a cylindrical wall and a flat bar (a three-dimensional illustration can be found later in figure 4). The heights of scoops were all 30 mm, while the opening diameters were 15 mm, 30 mm and 50 mm (corresponding to scoops from the smallest opening to the largest with ID of 1–3). The flat bar had a constant dimension (15 × 60 mm). Geometrical parameters of each tool can be found in table 1.

The additive technique used is similar to fused filament fabrication (FFF) [40,41]. With this technique, various structures can be automatically manufactured with the same robot arm by depositing fluidic TPA under preprogrammed nozzle trajectories in a layered-up manner. The trajectories of the nozzle for all the tools were preloaded into the Matlab program. With a horizontal speed of the nozzle at 1.5 mm s^{-1}, a bead width [42] of 1.5 mm can be obtained stably. A higher speed will result in discontinuity in manufactured structures, whereas a lower speed will make TPA beads too thick to provide a fine structure.

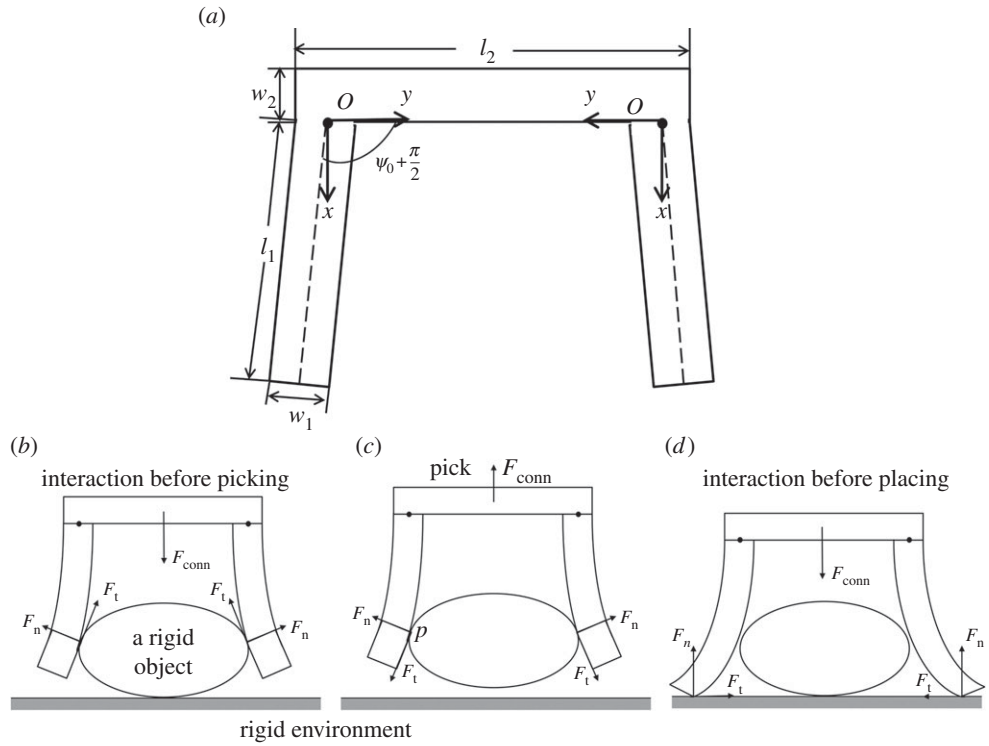

Figure 3. A solid-mechanics model of pick-and-place with a passive fingered gripper. (*a*) A two-dimensional passive gripper and its geometrical representation. The gripper is assumed to be symmetrical and massless. The top bar is assumed to be rigid. Pick-and-place with the gripper can be described as a finite state machine with four states. Three of the four states are (*b*) interaction before picking, (*c*) picking and (*d*) interaction before placing. The fourth state is placing which is trivial. Forces on the gripper involved in each state are indicated: F_{conn} is the connection force given by the bond with the TC, F_n is the normal contact force exerted by the rigid object and F_t is the tangential contact force exerted by the object.

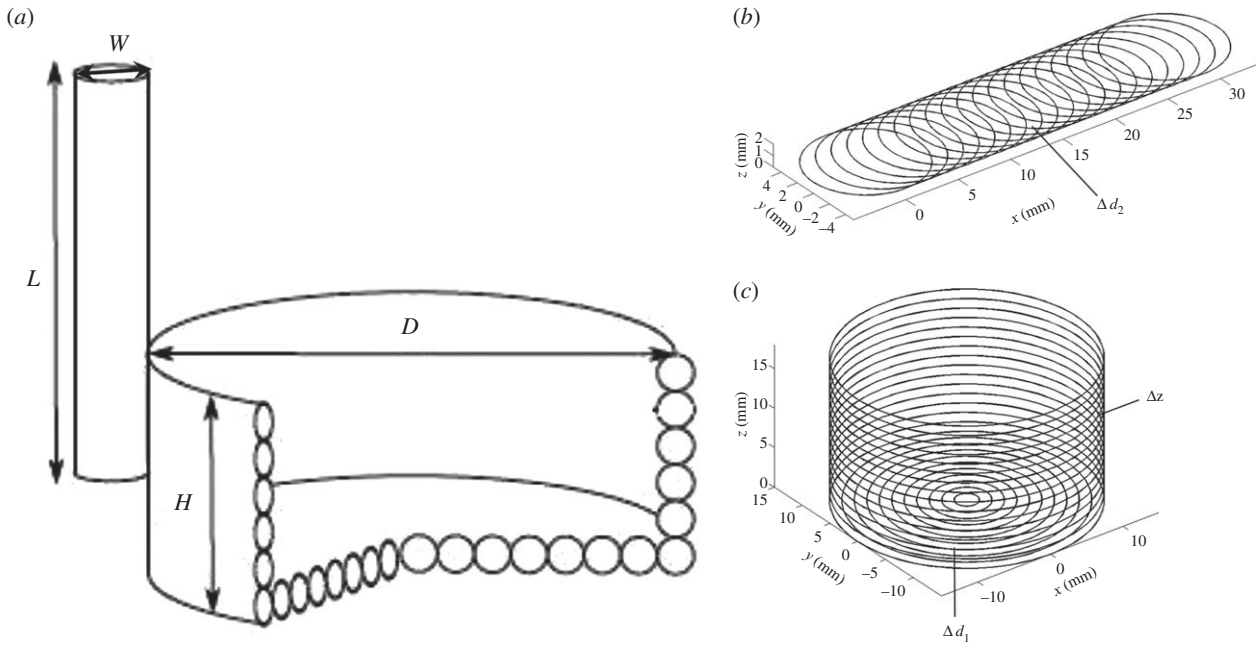

Figure 4. A scoop tool and its manufacturing process. (*a*) The scoop tool can be described by four geometrical parameters which are opening diameter *D*, height *H*, length and width of the handle bar *L* and *W*, respectively. (*b*) The trajectory in a layered manner for manufacture of the handle bar, and the combination of the bottom disc and the cylindrical wall.

After being manufactured, all the tools would be attached to TC by the robot itself through an open-loop heating and cooling process of TPA which took 140 s (refer to §2.1). The thermal adhesion makes the integration much easier and more flexible [38] than previous technologies, where manufactured structures had to be manually assembled [41,43], or alignment and interlocking mechanisms had to be added to structures during manufacture [44].

Table 1. Geometric parameters of the tools.

gripper	finger length l_1 (mm)	finger width w_1 (mm)	finger initial angle ψ_0	top bar length l_2 (mm)
1	15	3	0°	7
2	20	5	0°	20
3	55	5	15°	20
scoop	**opening diameter D (mm)**		**height H (mm)**	
1	15		30	
2	30		30	
3	50		30	

2.4. A solid-mechanics model of pick-and-place with a passive fingered gripper

A passive fingered gripper can pick and place rigid objects because its compliance enables deformation during physical interactions. To pick an object, the gripper can be opened by force insertion from the object, and closure may be achieved by force closure from friction and retraction. To place an object, the passive gripper must re-open, and this could be achieved either by fixing the object in the environment or by forces from the environment. Therefore, pick-and-place with a passive gripper can be, in the simplest form, described as a finite state machine with four states. As formulated in [45], there are two states of different physical interactions before the state of picking and the state of placing.

Here, we use a quasi-static two-dimensional gripper model. As illustrated in figure 3*a*, the gripper has two fingers that are symmetrically connected to a horizontal rigid bar on the top. Each finger has a length of l_1 and a width of w_1, and the top horizontal bar has a length of l_2 and a width of w_2. It is assumed that the third dimension of the gripper is homogeneous and has the same thickness (denoted as t) everywhere. The angle between the initial neutral axis of the finger (in a dashed line) and the bar is $\psi_0 + \pi/2$. It is assumed that the structure is massless. Figure 3*b–d* illustrates three of the four aforementioned states without the fourth state of placing. The local coordinates for each finger originate at point O. The positive direction of x-axis at the local coordinates is parallel to the approaching direction of the gripper towards the rigid object. The opening and closure of the gripper during the physical interaction before picking (figure 3*b*) and placing (figure 3*d*) may be modelled based on the contact model in [46]. Below the state of picking (figure 3*c*) is modelled.

Given a certain relative position between the gripper and the object, the contact point can be assumed as being the same and it is denoted as $\boldsymbol{P}_c$. Therefore, the maximal weight of any objects that may be picked in that position can be determined. By assuming the angle of rotation at the origin point O during picking is $\psi(0)^P$, as the top bar is rigid, the contact force during picking can be obtained from

$$E_1 I_1 \frac{\psi(0)^P - \psi_0}{\mathrm{d}s} = -\boldsymbol{P}_c \times \boldsymbol{F}^P, \tag{2.1}$$

where E_1 is Young's modulus of the material of the finger, $I_1 = tw_1^3/12$ is the second moment of area of the finger, $\boldsymbol{P}_c = [x_c, y_c]^T$ is the location vector from O to the contact point, and $\boldsymbol{F}^P = \boldsymbol{F}_n^P + \boldsymbol{F}_t^P = [F_{nx}^P, F_{ny}^P]^T + [F_{tx}^P, F_{ty}^P]^T$ is the contact force vector during picking, which consists of a normal vector and a tangential vector. As figure 3*c* illustrates, while the direction of the normal contact force maintains, the direction of the tangential force reverses, and it holds that

$$2F_{tx}^P = -(F_{conn} + 2F_{nx}^P) = -(W + 2F_{nx}^P). \tag{2.2}$$

In order for the object to be static with respect to the gripper, $F_t{}^P \le \mu_s F_n{}^P$ must be satisfied, where μ_s is the coefficient of static friction between the material of the finger and the material of the rigid object. Therefore, the maximal weight of the object is

$$W_{max} = -2(F_{tx}^P + F_{nx}^P) = -2(\mu_s F_n^P \cos\theta_c^P + F_n^P \sin\theta_c^P), \tag{2.3}$$

where θ_c^P is the contact angle of the finger (angle at the contact point) with respect to x-axis, and $|F_n^P| = \sqrt{|F^P|^2/(1+\mu_s^2)}$. Equation (2.3) indicates the maximal weight that can be picked and held is determined by the deflection of the fingers at the origin O, the contact angle and the coefficient of static friction, assuming the same modulus and geometrical parameters.

2.5. An energetic-cost model of tool manufacture

In general, energetic cost (CE_c) can be seen as the product of the time cost (CT_c) and average power consumption (PW_c)

$$CE_c = CT_c \cdot PW_c. \tag{2.4}$$

The time cost of manufacture is determined by the size and complexity of a structure [47,48] and average manufacturing speed, while power consumption depends on individual systems.

In the case of additive manufacturing, the size influences the total length of nozzle deposition trajectories and the complexity determines the number of parts of a structure that need to be combined. Hence the time cost of manufacture is the sum of the time cost of nozzle deposition (NDT) and of addition/combination (AT)

$$CT_c = NDT + AT. \tag{2.5}$$

Suppose a structure has N parts, and the time cost of nozzle deposition of the nth part is denoted NDT_n. NDT_n can be seen as the product of time needed to manufacture one layer and the number of layers NL_n for the nth part. The time needed for one layer can be further seen as the ratio between the path length on one layer PL_n and nozzle's deposition speed v. Therefore,

$$NDT = \sum_{n=1}^{N} NDT_n = \sum_{n=1}^{N} NL_n \cdot \frac{PL_n}{v} \tag{2.6}$$

and

$$AT = (N-1) \cdot OA. \tag{2.7}$$

In the special case of scoop manufacture, assuming all the three parts ($N = 3$) are thin, the scoop may be parametrized with four geometrical parameters (as illustrated in figure 4*a*): the opening diameter D, the height H, the length and width of the bar L and W, respectively. Given certain distance between

neighbouring filaments in the FFF technique, the path length on one layer PL_n for each part can be determined as

$$\left.\begin{aligned} PL_{1(disc)} &= \sum_{j=1}^{k_{disc}} 2\pi \cdot j \cdot \Delta d_1 = \pi \cdot \Delta d_1 \cdot k_{disc} \cdot (1 + k_{disc}), \\ PL_{2(wall)} &= \pi \cdot D \\ \text{and} \quad PL_{3(bar)} &= \pi \cdot W \cdot k_{bar}, \end{aligned}\right\} \tag{2.8}$$

where $k_{disc} = [D/2\Delta d_1]$, $k_{bar} = [(L - W)/\Delta d_2]$, with Δd_1 and Δd_2 being the distances between neighbouring filaments for the bottom disc and the bar (as illustrated in figure 4*b*). Given certain incremental height between layers in the FFF technique, the number of layers NL_n for each part can also be determined

$$\left.\begin{aligned} NL_{1(disc)} &= 1, \\ NL_{2(wall)} &= \left[\frac{H}{\Delta z}\right] \\ \text{and} \quad NL_{3(bar)} &= 1, \end{aligned}\right\} \tag{2.9}$$

where Δz is the incremental height between layers for the cylindrical wall (as illustrated in figure 4*b*).

2.6. Experiment

To evaluate the effectiveness of controlling objects and to verify the solid-mechanics model, we carried out the experiment with four of the six manufactured tools, i.e. gripper 1, gripper 2 and gripper 3, and scoop 1. The experiment consisted of a total of 480 runs, where the robot repeated 30 runs for each of the 16 combinations of the four tools and the four objects.

A single fixed trajectory was predefined for the robot to use tools to pick and place fluid and solid objects. More specifically, objects were positioned in a predefined location in the motor task space. The robot arm picked and transported each object (excluding the container or the tray in the case of water or rice grains) over a given horizontal distance (200 mm) and then placed them at another predefined location in the motor task space. As visualized in figure 5, the trajectory consists of eight segments. The first and second segments are vertical down- and up-strokes along the *x*-axis above the pick position. These motion segments either induced 'scooping' in the case with water, or resulted in 'passive gripping' in the cases with solid objects. After a translation motion along the *y*-axis (the third motion segment), the fourth motion segment contains a rotational motion. With the scoop containing water, this motion segment induces 'pouring' of the water at the place position, whereas it gives no effect on solid objects. The fifth and sixth motion segments allow grippers to open the fingers and release the transported objects when they are pushed against the ground. By contrast, these motion segments do not have any influence on the liquid. The last two segments move the robot back to the initial position or to start a new repetition of pick-and-place. Table 2 gives a list of actions taken in each segment of the trajectory. Execution of the entire trajectory took 18 s.

We collected quantitative data as follows for effectiveness evaluation: in the case of water, we measured the mass of the water transported and remained in the container at the place position; for rice grains, we counted the number of pieces that remained in the place position; and when the pebble and the plastic box were transported, we simply counted the successful cases when the object was at the place location in the end. Experimental results with solid objects were compared to the solid-mechanics model as described in §2.4. The maximal possible mass that was able to be picked by each gripper for a given contour of the object and coefficient of friction was analysed. To measure the maximal mass in the experiment, metal blocks of various known mass of 1–20 g were added incrementally to the three solid objects after they had been picked up and statically held by the grippers until failure. Specifically, the metal blocks were attached to the rice grain or pebble through a string of TPA, or they were put inside the plastic box. In this way, the contour and the coefficient of friction for each solid object could be maintained while the mass could be easily varied. Theoretical values of the maximal holding mass in the three cases with the three grippers were estimated based on the solid-mechanics model in §2.4, with the contact point, the contact angle and the deflection of the finger at the origin obtained from image analysis using standard edge detectors in Matlab.

To analyse the energetics of tool manufacture and use, we first compared the energetic cost between the three scoops in Matlab simulation to show possible reduction of the cost when

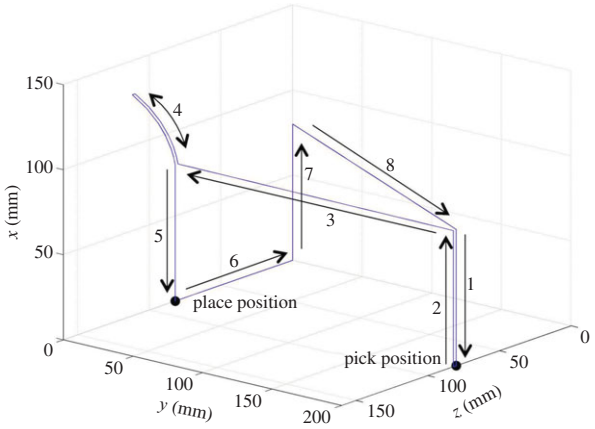

Figure 5. A predefined fixed trajectory of the end effector for pick-and-place of all objects in a three-dimensional view. (1) Every pick-and-place experiment starts with the end-effector of the robot arm placed above the pick position, and it moves down vertically. (2) After the down-stroke, the end-effector moves back up vertically. (3) The end-effector is translated horizontally to the location above the place position. (4) Over the place position, the end-effector is inclined forward with a small rotation angle. (5) The end-effector is moved down vertically at the place location. (6) While maintaining the lower vertical position, the robot arm shifts the end-effector backward. (7 and 8) Finally, the end-effector moves back up and goes back to the initial position. (Online version in colour.)

Table 2. Segments of the trajectory and their corresponding actions.

segment	action
1	vertical downward motion (along *x*-axis) before picking
2	vertical upward motion (along *x*-axis) after picking
3	horizontal motion (along *y*-axis) for transportation
4	rotational motion (about *y*-axis) for placing water, no effect on solid objects
5	vertical downward motion (along *x*-axis) before placing solid objects
6	horizontal motion (along *z*-axis) for placing solid objects
7	vertical upward motion (along *x*-axis) after placing solid objects
8	horizontal motion (along *y*-axis) for returning to the initial position

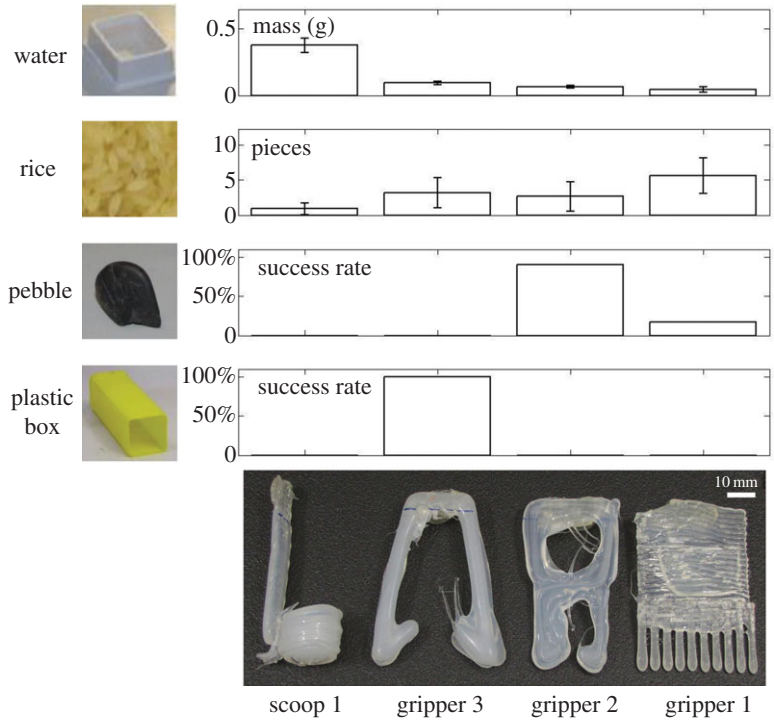

Figure 6. Experiment results in pick-and-place of four objects with four tools, all under the same motor trajectory shown in figure 5. Photos of the four objects and four tools are added to show their significant difference in physical properties, shapes and sizes. (Online version in colour.)

picking and placing water of 30, 300 and 1300 g. Specifically, the energetic cost of manufacture was estimated based on experimentally recorded time for the three scoops multiplied by the power consumption of manufacture PW_c. PW_c equals 435 W which includes the apparent power of the robot and the TPA Supplier (see §2.1), whereas the power of the Peltier element is negligible. The energetic cost of tool use was estimated as the product of required numbers of repetition of pick-and-place for a certain mass, the time of each repetition (18 s, see above) and the power consumption of pick-and-pace (which is the apparent power of the robot, 420 W). Secondly, we implemented the energetic-cost model in the simulation for scoops with a wider range of opening diameters and heights in pick-and-place the three masses of water.

3. Results

The result of the pick-and-place experiment is shown in figure 6, with photos of the four objects and the four tools are added on the side (also see the electronic supplementary material, video). Specifically, scoop 1 transported an average of 0.376 g of water with a standard deviation of 0.055 g, gripper 2 transported the pebble with a 90% success rate and gripper 3 transported the plastic box with a 100% success rate. In terms of rice grains, gripper 1 transported an average of 5.6 pieces of rice with a standard deviation of 2.6 pieces. The results show that the water, pebble and plastic box could only be picked and placed by certain passive tools. The other tools happened to pick and place a small amount of rice grains which gripper 1 was better at. That is most probably due to the un-modelled adhesion forces from, for example, surface energy between the TPA and rice grains. Overall, the result suggests that even with a single series of motor command, manufactured passive tools could enable the robot arm to effectively pick and place fluid and dimensionally different solid objects.

Figure 7 shows the result in verification of the solid-mechanics model. The model predicts the maximal mass of solid objects that could be held by passive grippers, given a specific contour and material of the object as well as the contact point. The figure shows the maximal mass of the three solid objects that their pairing grippers could pick up and hold. Estimated values of the maximal mass from the mathematical model are also plotted, which are based on measured values for deflection and contact points as summarized in table 3. It can be seen that, a maximal mass of over 30 g was achieved for the pebble and the plastic box, whereas for the rice grain a maximal mass of just under 5 g could be held. The matching between experimental and estimated values in the analysis also shows that the mechanism of pick-and-place with fingered gripper tools can be explained by the mathematical model.

Regarding energetics of manufacturing and using tools of different sizes, manufacture of a larger scoop incurs more energetic cost because it takes longer to make. Experimental results show that with the same power assumption of 435 W, manufacture of scoop 1, 2 and 3 (small to large in terms of opening diameter) required a duration of 1571, 2747 and 4739 s, respectively. However, when the mass of water changes, a bigger scoop may reduce the number of pick-and-place repetitions, thus change in scoop dimension may actually reduce the total energetic cost.

Figure 8 shows calculation with three masses of water. When 30 g of water is to be fetched, it would need approximately 736 KJ to manufacture and use the small scoop 1 with seven repetitions of pick-and-place, while it would need approximately 2069 KJ to manufacture and use the big scoop 3 with one repetition of pick-and-place. When 1300 g of water is to be fetched, it would need 2679 KJ to manufacture and use the small scoop 1 with 264 repetitions of pick-and-place which is a significant increase, but the energy needed for big scoop 3 increases only a little (2243 KJ and 24 repetitions of pick-and-place) and it turns out to be less than

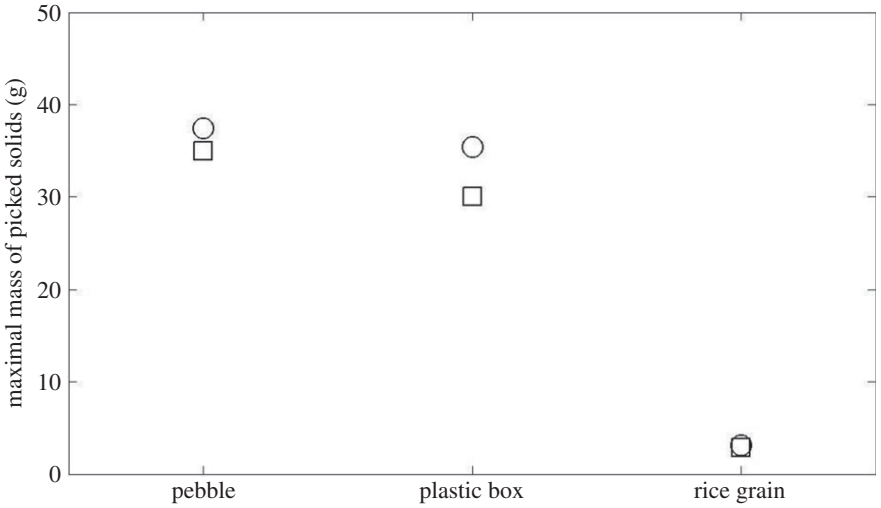

Figure 7. Analysis of experimental results related to the grippers in terms of maximal holding weight of the three solid objects. Estimated values are calculated from measured deflection parameters based on the mathematical model as presented in §2.4. The matching results show that the mathematical model explains the mechanism of pick-and-place with passive fingered gripper tools. Circles represent estimated value and squares, experimental result.

Table 3. Measured values of fingered grippers holding the three rigidly solid objects. ds = 3 mm, E_1 = 10 MPa.

gripper	object	μ_s	$\psi(0)^p$ (rad)	P_c (mm)	θ_c^p
1	rice grain	1.30	0.015	[11, −0.8]	4.5°
2	pebble	0.45	0.019	[20.6, −3.75]	30.3°
3	plastic box	0.75	0.017	[43, −19]	27.8°

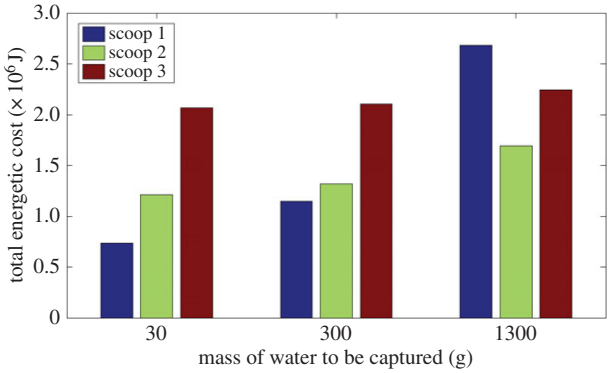

Figure 8. Total energetic cost of the manufacture and use of the three scoop tools for three mass of water (30, 300 and 1300 g). (Online version in colour.)

Table 4. Simulation values for the energetic-cost model of manufacturing scoop tools.

Δd_1	1.5 mm
Δd_2	1.5 mm
Δz	1.2 mm
OA	60 s
v	1.5 mm s^{-1}

scoop 1. This calculation shows plasticity in manufactured tools could be advantageous under certain circumstances as compared to manufacturing and using a fixed tool.

Further simulation results based on the energetic-cost model (see §2.5) and parameters in table 4 suggests which geometrical values of scoops would give the least total energetic cost of manufacture and use for a certain mass of water. Figure 9 shows the total energetic cost for a range of opening diameters and heights of the scoop with the length and width of the bar part being constant. In figure 9*a*, the height of the scoop is set to 30 mm, and three curves show the relation between the total energetic cost and opening diameter. The minimal point is indicated with a circle on each curve, corresponding to an opening diameter of 23.4, 49.4 and 59.3 for 30, 300 and 1300 g of water, respectively. In figure 9*b*, the opening diameter of the scoop is set to 30 mm, and the three curves show the relation between the total energetic cost and height. The minimal point corresponds to a height of 23, 45.7 and 94.5 mm for the three mass of water. The figure delivers the following two messages: firstly, the optimal values of D and H increase with the mass of water to be fetched. Secondly, plasticity in the tools becomes more crucial as the mass of water increases because the total energetic cost can be orders of magnitude smaller. For example, as figure 9*a* shows, instead of spending over nearly 10 000 KJ on transporting 1300 g water, the robot can spend just above 500 KJ with an optimal D = 59.3 mm of the scoop. It is worth mentioning that the curves in figure 9 show 'jumps' because the number of repetitions changes in a discrete way with continuous change of geometrical parameters.

4. Discussion

The fact that plasticity in tool manufacture and use incurs additional energetic costs may seem a reason why tool

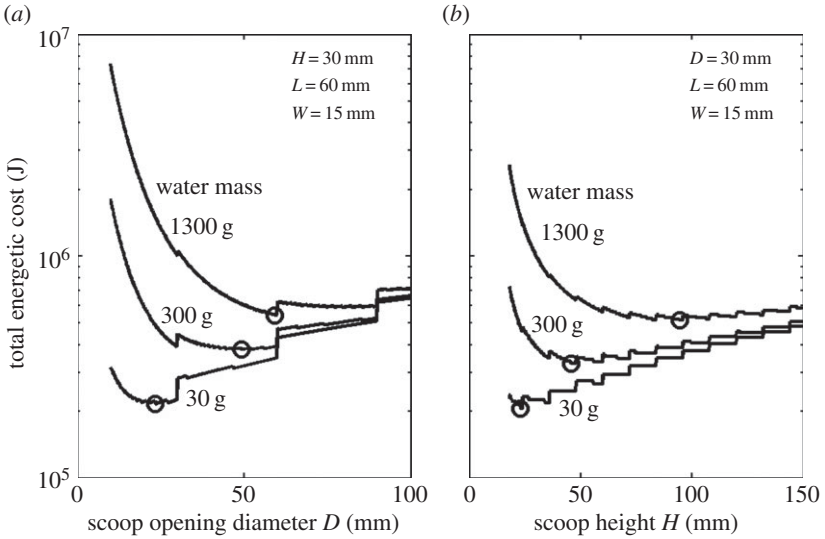

Figure 9. Total energetic cost of the manufacture and use of scoops with different geometrical values for three mass of water (30, 300 and 1300 g). (*a*) Different opening diameter; (*b*) Different height. The optimal value for the least total energetic cost is indicated by a circle in each case.

manufacture is rarer than mere tool use in the animal kingdom [49]. The results here show that plasticity in tool manufacture and use could be beneficial to animal users in at least two ways. Firstly, by modifying tools, a wider range of objects could be handled effectively with little change in motor control. The biomechanics behind this is that the morphology of passive tools off-loads some of the work that would have been done by motor control at the neuronal level. Secondly, under certain circumstances where a large amount of objects need to be handled, changing the dimension of tools could reduce the number of repetitions and, therefore, reduce the total energetic cost of tool manufacture and use.

The synthetic approach provides a way to do quantitative study of biomechanics in tool manufacture and use. Similarity between the robot model and animals lies in that tools are passive and tool manufacture involves movements of body parts such as arms in the robot and primates or mouths in birds, etc., although the level of handling material in animals may not be as high as that in the robot. The study presented here focused on two modes of tool manufacture (add/combine mode and reshape mode) and one of the tool use functions (i.e. effective control of fluids and solid objects), however, the approach may be extended to study detach mode and subtract mode of tool manufacture for other functions such as force amplification and extension of reaching.

The presented work also provides a way to formulate and analyse energetic cost of tool manufacture and use. The limitation is that it does not have analysis of all kinds of energetic costs, due to the fact that the robot is constrained by its mobility and functionality. Thus, other production-associated costs cannot be analysed such as costs of travelling and collecting source material (see §1). Besides production-associated costs, other costs such as maintenance costs [17] cannot be analysed with the physical model due to the lack of sensors. Future work may use a mobile model with onboard sensors for further analysis.

The tools have to be 'designed' or 'optimized' by the animal somehow so that they can physically interact in certain ways with objects. This is clearly a manifestation of complex cognition [50]. However, whether it is an indication of the higher level of intelligence than related species remains arguable as: (i) the exact cognitive mechanisms underlying tool manufacture and use remain unknown; (ii) tool-manufacturing animals do not consistently outperform non-tool using related species in problem-solving tasks in the laboratory and (iii) seemingly sophisticated behaviour comparatively can be also generated by simple processes.

Besides its implication to biological study, the presented work may also shed light on designing so-called morpho-functional machines [51]. The concept essentially designates that as functions such as locomotion, grasping and reaching are the results of physical system–environment interactions, the shapes and their dynamic material properties are as essential as the neuronal control of motions, and it is necessary to systematically investigate the morphology in the context of adaptive behaviours [52]. Previously, multi-functionality in machines through morphological change has been demonstrated with modular robotic systems, where wheeled and legged structures could be automatically generated from the same set of robotic modules for locomotion on flat and rugged surfaces [53]. There have been some robots that could use simple tools [2,54,55], but none could both manufacture and use tools. The results prove that by making different passive tools from source material which is a behaviour inspired by some animals, a robotic system can vary the morphology of an extended structure to realize morpho-functions. The demonstration of the new approach opens the possibility of further research topics, such as identification of important material properties with other types of source material such as foams [56], as well as technical improvement in design optimization and automation. For example, design optimization may be achieved by mounting vision sensors on the robot to detect the contour of the object and feeding sensory information back to a high-level simulator implementing solid-mechanics models such as the one described in §2.4; and design automation may be achieved a step further by the robot with a higher level function based on, for example, evolutionary computation [43,57].

Funding statement. The work was supported by the Swiss National Science Foundation Professorship grant no. PP00P2123387/1, and the ETH Zurich Research grant ETH-23-10-3.

References

1. Bentley-Condit VK, Smith EO. 2010 Animal tool use: current definitions and an updated comprehensive catalog. *Behaviour* **147**, 185–221. (doi:10.1163/000579509X12512865686555)
2. Shumaker RW, Walkup KR, Beck BB. 2011 *Animal tool behavior: the use and manufacture of tools by animals*. Baltimore, MD: Johns Hopkins University Press.
3. Chappell J, Kacelnik A. 2002 Tool selectivity in a non-mammal, the New Caledonian crow (*Corvus moneduloides*). *Anim. Cogn.* **5**, 71–78. (doi:10.1007/s10071-002-0130-2)
4. Hansell M. 2005 *Animal architecture*. Oxford, UK: Oxford University Press.
5. Bird CD, Emery NJ. 2009 Insightful problem solving and creative tool modification by captive nontool-using rooks. *Proc. Natl Acad. Sci. USA* **106**, 10 370–10 375. (doi:10.1073/pnas.0901008106)
6. Price EE, Lambeth SP, Schapiro SJ, Whiten A. 2009 A potent effect of observational learning on chimpanzee tool construction. *Proc. R. Soc. B* **276**, 3377–3383. (doi:10.1098/rspb.2009.0640)
7. St Clair JJH, Rutz C. 2013 New Caledonian crows attend to multiple functional properties of complex tools. *Phil. Trans. R. Soc. B* **368**, 20120415. (doi:10.1098/rstb.2012.0415)
8. Lethmate J. 1977 Instrumentelles Verhalten zoolebender Orang-Utans. *Z. Morph. Anthrop.* **68**, 57–87.
9. Dawkins R. 1982 *The extended phenotype*. Oxford, UK: W. H. Freeman.
10. Pigliucci M. 2001 *Phenotypic plasticity: beyond nature and nurture*. Baltimore, MD: John Hopkins University Press.
11. Hunt GR. 2000 Human-like, population-level specialization in the manufacture of pandanus tools by the New Caledonian crows *Corvus moneduloides*. *Proc. R. Soc. Lond. B* **267**, 403–413. (doi:10.1098/rspb.2000.1015)
12. Hunt GR. 1996 Manufacture and use of hook-tools by New Caledonian crows. *Nature* **379**, 249–251. (doi:10.1038/379249a0)
13. Chappell J, Kacelnik A. 2004 Selection of tool diameter by New Caledonian crows *Corvus moneduloides*. *Anim. Cogn.* **7**, 121–127. (doi:10.1007/s10071-003-0202-y)
14. van Schaik CP, Fox EA, Sitompul AF. 1996 Manufacture and use of tools in wild Sumatran orangutans. *Naturwissenschaften* **83**, 186–188. (doi:10.1007/BF01143062)
15. Auld JR, Agrawal AA, Relyea RA. 2010 Re-evaluating the costs and limits of adaptive phenotypic plasticity. *Proc. R. Soc. B* **277**, 503–511. (doi:10.1098/rspb.2009.1355)
16. van Kleunen M, Fischer M. 2005 Constraints on the evolution of adaptive phenotypic plasticity in plants. *New Phytol.* **166**, 49–60. (doi:10.1111/j.1469-8137.2004.01296.x)
17. DeWitt TJ, Sih A, Wilson DS. 1998 Costs and limits of phenotypic plasticity. *Trends Ecol. Evol.* **13**, 77–81. (doi:10.1016/S0169-5347(97)01274-3)
18. Aoi S, Katayama D, Fujiki S, Tomita N, Funato T, Yamashita T, Senda K, Tsuchiya K. 2013 A stability-based mechanism for hysteresis in the walk–trot transition in quadruped locomotion. *J. R. Soc. Interface* **10**, 20120908. (doi:10.1098/rsif.2012.0908.)
19. Curet OM, Patankar NA, Lauder GV, MacIver MA. 2011 Aquatic manoeuvering with counter-propogating waves: a novel locomotive strategy. *J. R. Soc. Interface* **8**, 1041–1050. (doi:10.1098/rsif.2010.0493)
20. Elzinga MJ, Dickson WB, Dickinson MH. 2012 The influence of sensory delay on the yaw dynamics of a flapping insect. *J. R. Soc. Interface* **9**, 1685–1696. (doi:10.1098/rsif.2011.0699)
21. Libby T, Moore YM, Chang-Siu E, Li D, Cohen DJ, Jusufi A, Full RJ. 2012 Tail-assisted pitch control in lizards, robots and dinosaurs. *Nature* **481**, 181–184. (doi:10.1038/nature10710)
22. Li C, Zhang T, Goldman DI. 2013 A terradynamics of legged locomotion on granular media. *Science* **339**, 1408–1412. (doi:10.1126/science.1229163)
23. Maladen RD, Ding Y, Umbanhowar PB, Kamor A, Goldman DI. 2011 Mechanical models of sandfish locomotion reveal principles of high performance subsurface sand-swimming. *J. R. Soc. Interface* **8**, 1332–1345. (doi:10.1098/rsif.2010.0678)
24. Ijspeert AJ, Crespi A, Ryczko D, Cabelguen J-M. 2007 From swimming to walking with a salamander robot driven by a spinal cord model. *Science* **315**, 1416–1420. (doi:10.1026/science.1138353)
25. Owaki D, Kano T, Nagasawa K, Tero A, Ishiguro A. 2013 Simple robot suggests physical interlimb communication is essential for quadruped walking. *J. R. Soc. Interface* **10**, 20120669. (doi:10.1098/rsif.2012.0669)
26. Webb B. 2002 Robots in invertebrate neuroscience. *Nature* **417**, 359–363. (doi:10.1038/417359a)
27. Krink T, Vollrath F. 1998 Emergent properties in the behaviour of a virtual spider robot. *Proc. R. Soc. Lond. B* **265**, 2051–2055. (doi:10.1098/rspb.1998.0539)
28. Bongard JC. 2011 Morphological change in machine accelerates the evolution of robot behavior. *Proc. Natl Acad. Sci. USA* **108**, 1234–1239. (doi:10.1073/pnas.1015390108)
29. Li W, Bouzidi L, Narine SS. 2008 Current research and development status and prospect of hot-melt adhesives: a review. *Ind. Eng. Chem. Res.* **47**, 7524–7532. (doi:10.1021/ie800189b)
30. Schmidt H, Scholze H, Tnker G. 1986 Hot melt adhesives for glass containers by the sol-gel process. *J. NonCryst. Solids* **80**, 557–563. (doi:10.1016/0022-3093(86)90446-1)
31. Park Y-J, Kim H-J. 2003 Hot-melt adhesive properties of EVA/aromatic hydrocarbon resin blend. *Int. J. Adhes. Adhes.* **23**, 383–392. (doi:10.1016/S0143-7496(03)00069-1)
32. Clevy C, Hubert A, Agnus J, Chaillet N. 2005 A micromanipulation cell including a tool changer. *J. Micromech. Microeng.* **15**, S292–S301. (doi:10.1088/0960-1317/15/10/S07)
33. Boehm S, Dilger K, Hesselbach J, Wrege J, Rathmann S, Ma W, Stammen E, Hemken G. 2006 Micro bonding with non-viscous adhesives. *Microsyst. Technol.* **12**, 676–679. (doi:10.1007/s00542-006-0101-7)
34. Rathmann S, Schoettler K, Berndt M, Hemken G, Raatz A, Tutsch R, Boehm S. 2008 Sensor-guided micro assembly of active micro systems by using a hot melt based joining technology. *Microsyst. Technol.* **14**, 1975–1981. (doi:10.1007/s00542-008-0681-5)
35. Matsumoto M, Hashimoto S. 2009 Passive self-replication of millimeter-scale parts. *IEEE Trans. Autom. Sci. Eng.* **6**, 385–391. (doi:10.1109/TASE.2008.2006625)
36. Wang L, Graber L, Iida F. 2013 Large-payload climbing in complex vertical environments using thermoplastic adhesive bonds. *IEEE Trans. Robot.* **29**, 863–874. (doi:10.1109/TRO.2013.2256312)
37. Wang L, Culha U, Iida F. 2014 A dragline-forming mobile robot inspired by spiders. *Bioinspir. Biomim.* **9**, 016006. (doi:10.1088/1748-3182/9/1/016006)
38. Wang L, Iida F. 2012 Physical connection and disconnection based on hot-melt adhesives. *IEEE-ASME Trans. Mechatron.* **18**, 1397–1409. (doi:10.1109/TMECH.2012.2202558)
39. Brodbeck L, Wang L, Iida F. 2012 Robotic body extension based on hot melt adhesives. In *Proc. IEEE ICRA 2012, 14–18 May, St Paul, MN*, pp. 4322–4327. New York, NY: IEEE Press.
40. Crump S. 1991 Fused deposition modeling (FDM): putting rapid back in prototyping. In *Proc. 2nd Int. Conf. Rapid Prototyping, 23–26 June, Dayton, OH*, pp. 358–361. Dayton, OH: University of Dayton.
41. Jones R, Haufe P, Sells E, Iravani P, Oliver V, Palmer C, Bowyer A. 2011 RepRap—the replicating rapid prototyper. *Robotica* **29**, 177–191. (doi:10.1017/S026357471000069X)
42. Sabourin E, Houser SA, Bohn JH. 1996 Adaptive slicing using stepwise uniform refinement. *Rapid Prototyping J.* **2**, 20–26. (doi:10.1108/13552549610153370)
43. Lipson H, Pollack JB. 2000 Automatic design and manufacture of robotic lifeforms. *Nature* **406**, 974–978. (doi:10.1038/35023115)
44. Moses MS, Yamaguchi H, Chirikjian GS. 2010 Towards cyclic fabrication systems for modular robotics and rapid manufacturing. In *Robotics, science and systems V* (eds J Trinkle, Y Matsuoka, JA Castellanos). Cambridge, MA: MIT Press.
45. Sakai S, Nakamura Y, Nonami K. 2007 A pick-and-place hand mechanism without any actuators and sensors. In *Proc. IEEE ICRA 2007, 10–14 April, Rome, Italy*, pp. 4064–4070. New York, NY: IEEE Press.
46. Lan C-C, Lee K-M. 2008 An analytical contact model for design of compliant fingers. *J. Mech. Des.* **130**, 011008. (doi:10.1115/1.2803655)
47. Gutowski T, Hoult D, Dillon G, Neoh E-T, Muter S, Kim E, Tse M. 1994 Development of a theoretical

cost model for advanced composite fabrication. *Compos. Manuf.* **5**, 231–239. (doi:10.1016/0956-7143(94)90138-4)

48. Apostolopoulos P, Kassapoglou C. 2002 Recurring cost minimization of composite laminated structures optimum part size as a function of learning curve effects and assembly. *J. Compos. Mater.* **36**, 501–518. (doi:10.1177/0021998302036004556)
49. Ruston GD, Hansell MH. 2009 Why are pitfall traps so rare in the natural world? *Evol. Ecol.* **23**, 181–186. (doi:10.1007/s10682-007-9218-0)
50. Emery NJ, Clayton NS. 2004 The mentality of crows: convergent evolution of intelligence in corvids and apes. *Science* **306**, 1903–1907. (doi:10.1126/science.1098410)
51. Hara F, Pfeifer R. 2003 *Morpho-functional machines: the new species*. Tokyo, Japan: Springer.
52. Pfeifer R, Lungarella M, Iida F. 2007 Self-organization, embodiment, and biologically inspired robotics. *Science* **318**, 1088–1093. (doi:10.1126/science.1145803)
53. Stoy K, Brandt D, Christensen DJ. 2010 *Self-reconfigurable robots: an introduction*. Cambridge, MA: MIT Press.
54. Stoytchev A. 2005 Behavior-grounded representation of tool affordances. In *Proc. IEEE ICRA 2005*, *18–22 April, Barcelona, Spain*, pp. 3060–3065. New York, NY: IEEE Press.
55. Nabeshima C, Kuniyoshi Y, Lungarella M. 2006 Adaptive body schema for robotic tool-use. *Adv. Robot.* **20**, 1105–1126. (doi:10.1163/156855306778522550)
56. Revzen S, Bhoite M, Macasieb A, Yim M. 2011 Structure synthesis on-the-fly in a modular robot. In *Proc. IEEE/RSJ IROS 2011*, *25–30 September, San Francisco, CA*, pp. 4797–4802. New York, NY: IEEE Press.
57. Wang Y, Duarte JP. 2002 Automatic generation and fabrication of designs. *Autom. Constr.* **11**, 291–302. (doi:10.1016/S0926-5805(00)00112-6)